

CeO₂ and Mn₃O₄-based nanozymes exhibit scavenging of singlet oxygen species and hydroxyl radicals

Krishnendu M R^{a,b}, Divya Mehta^{a,b}, and Sanjay Singh^{a,b}*

^aNanobiology and Nanozymology Laboratory, National Institute of Animal Biotechnology (NIAB), Opposite Journalist Colony, Near Gowlidoddy, Extended Q-City Road, Gachibowli, Hyderabad, Telangana 500032, India.

^bRegional Centre for Biotechnology (RCB), Faridabad 121001, Haryana, India

*Corresponding author's address:

Dr. Sanjay Singh

Scientist F

DBT-National Institute of Animal Biotechnology (NIAB), Opposite Journalist Colony, Near Gowlidoddy, Extended Q-City Road, Gachibowli, Hyderabad – 500032, Telangana, India.

Email ID: sanjay@niab.org.in

Supporting Information

1. Dextran coated nanozyme synthesis method:

Dextran coated CeO₂ nanoparticles (Dex-CeO₂ NPs) were synthesized using the protocol described by Naha et al¹. In the formation of Dex-CeO₂ NPs, precipitation of cerium salts occurs with the addition of ammonium hydroxide in presence of dextran. Briefly, 0.5 ml of 1M cerium nitrate hexahydrate was dissolved in 2 ml of 0.008 M dextran solution. 3 ml of ammonium hydroxide (30%) solution was added to a preheated glass vial at 90°C. The dissolved mixture of cerium nitrate and dextran solution was then added dropwise to the ammonium hydroxide (30%) solution with stirring and allowed the reaction mixture to stir at 90°C for 1 h. The reaction mixture was cooled down to room temperature after 1 hour of heating and stirred for overnight. The synthesized Dex-CeO₂ NPs were dialyzed against Milli-Q water using a dialysis membrane (MWCO 12.5 kDa) for approximately

16 hours to bring the pH to 7.4. The purified Dex-CeO₂ NPs was used for ICPMS analysis and stored at 4°C for further use. Synthesis of Dex-Mn₃O₄ NPs was carried out based on chemical precipitation method ². In brief, 20 ml of 12 mM manganese (II) chloride hexahydrate was dissolved in 45 ml of 6mM dextran solution. The reaction mixture was heated at 80°C and 4.7 ml of 0.5 M NaOH was added to the reaction mixture with stirring. Brown colour suspension was formed instantly on addition of NaOH. The suspension was stirred for 1 hour at 80°C and cooled to room temperature with stirring for overnight. The synthesized Dex- Mn₃O₄ NPs was dialyzed against Milli-Q using dialysis membrane (M.W.-12.5 kDa) to neutralize the pH. The purified Dex- Mn₃O₄ NPs was used for ICPMS analysis and stored at 4°C for further use.

2. Characterization of nanozymes:

All characterization techniques were performed using purified Dex-CeO₂ NPs and Dex-Mn₃O₄ NPs. Absorbance spectra of dextran, Dex-CeO₂ NPs and Dex-Mn₃O₄ NPs was performed from a concentration of 300 µM by multimode reader (Synergy LX, BioTek) using 1ml quartz cuvette. Zeta potential of dextran, Dex-CeO₂ NPs and Dex-Mn₃O₄ NPs were analyzed using dynamic light scattering measurement (DLS) (Litesizer 500, Anton Paar). The size and shape of Dex-CeO₂ NPs and Dex-Mn₃O₄ NPs was determined by transmission electron microscope (TEM). For TEM imaging, 10 µl of the purified Dex-CeO₂ NPs and Dex-Mn₃O₄ NPs were loaded on a carbon coated copper grid and dried overnight under vacuum. The surface morphology and elemental composition of Dex-CeO₂ and Dex-Mn₃O₄ NPs were analyzed using a scanning electron microscope (SEM, EVO18, Carl Zeiss) coupled with an energy dispersive X-ray spectrometer (EDX, ELEMENT, AMETEK). Samples were prepared by loading the nanoparticles onto carbon-coated copper stubs, followed by gold sputter coating using a sputter coater (SC7620, Quorum) prior to imaging. The Fourier transform infrared (FT-IR) spectroscopy of dextran, Dex-CeO₂ NPs and Dex-Mn₃O₄ NPs were carried out by using FT-IR spectrometer (NICOLET iS50 FT-IR, ThermoScientific). For the FT-IR analysis, samples were dried with KBr powder in 2:1 ratio and analysed using attenuated total reflectance (ATR) mode in the range of 400– 4000 cm⁻¹. The phase identification and crystalline

structure of Dex-CeO₂ NPs and Dex-Mn₃O₄ NPs were obtained by X-Ray Diffraction (Bruker D8 Advance LYNXYE XE-T) analysis. XPS analysis was performed to determine the oxidation states and chemical composition of Dex-CeO₂ and Dex-Mn₃O₄ NPs. Measurements were carried out using an Axis Supra, X-ray photoelectron spectrometer (Shimadzu Group) equipped with an Al K α X-ray source. Survey spectra were recorded over the binding energy range of 0–1200 eV. High-resolution spectra for Ce 3d, Mn 2p, C 1s, and O 1s were acquired to analyze the elemental states. Peak fitting was performed using Gaussian curve fitting in Origin 2023b software.

3. Methods of generation and scavenging of hydroxyl radicals

The reaction system consists of 0.55 mM FeSO₄ and 1.58 mM H₂O₂ dissolved in 10mM tris buffer of pH 7. 2.5 mM terephthalic acid (TA) was added to the reaction system maintained to the total volume of 500 μ l and incubated for 15 minutes. After the incubation, the fluorescent emission intensity of TA at 425 nm was measured using the multimode reader (EnSpire, PerkinElmer) at excitation wavelength 320 nm. For the kinetics study, the reaction system of 500 μ l volume was prepared by adding all the reagents except H₂O₂. 1.58 mM H₂O₂ was added to the reaction system just before initiating the kinetics readings. The kinetics of the emission intensity of TA at 425 nm was measured for 20 minutes using the multimode reader (EnSpire, PerkinElmer) at an excitation wavelength, 320 nm.

3.1. Hydroxyl radical scavenging activity of Dex-CeO₂ NPs and Dex-Mn₃O₄ NPs.

The hydroxyl radicals (\cdot OH) scavenging activity of Dex-CeO₂ NPs and Dex-Mn₃O₄ NPs were carried out in a range of 5-200 μ M. 30 μ l from each stock solutions of Dex-CeO₂ NPs and Dex-Mn₃O₄ NPs corresponding to the concentration range under study were added to the reaction system consisting of 0.55 mM FeSO₄ and 1.58 mM H₂O₂ in tris buffer. After adding nanoparticles, the reaction system was incubated for 5 minutes. Following the incubation, TA (2.5mM) was added and the reaction system was incubated for 15 minutes. At the end of incubation, the emission intensity of TA was measured at 425 nm at an excitation wavelength of 320 nm using the multimode reader (EnSpire, PerkinElmer).

3.2. Evaluation of hydroxyl radical generation using inhibitors. 10% DMSO and 10% ethanol used as inhibitors of $\cdot\text{OH}$ were added respectively to individual 500 μl reaction systems consisting 0.55 mM FeSO_4 and 1.58 mM H_2O_2 in 10mM tris buffer. After 15 minutes of incubation, the emission intensity of TA at 425 nm was measured at an excitation wavelength, 320 nm using the multimode reader (EnSpire, PerkinElmer).

3.3. Reaction mechanism behind the scavenging of hydroxyl radical. The possible generation of molecular oxygen as an end product of $\cdot\text{OH}$ scavenging activity by the Dex- CeO_2 NPs and Dex- Mn_3O_4 NPs was studied using a dissolved oxygen (DO) meter (HANNA, edge dedicated Dissolved Oxygen, 230V - HI2004-02). 10 ml of the reaction system consisting FeSO_4 and H_2O_2 in tris buffer at pH 7 was incubated for 10 minutes to allow the generation of $\cdot\text{OH}$. After 10 minutes of incubation, 100 μM and 200 μM of Dex- CeO_2 NPs and Dex- Mn_3O_4 NPs were added respectively to the reaction mixture and was followed by measuring the dissolved oxygen level using a digital dissolved oxygen electrode in the reaction system maintained under stirring. Readings for the level of dissolved oxygen was recorded at an interval of every 30 seconds for 20 minutes.

The generation of H_2O_2 as a possible end product of the $\cdot\text{OH}$ scavenging activity of Dex- CeO_2 NsP and Dex- Mn_3O_4 NPs was investigated using amplex red assay. A master mix (2.5 mL) was prepared using 10mM Amplex[®] red reagent (10 μL), 1U/1 μl horseradish peroxidase (10 μL) and assay buffer (2.46 mL). 50 μL of supernatant of each reaction system used for assaying the $\cdot\text{OH}$ scavenging activity of the nanoparticles at concentrations, 100 μM and 200 μM was mixed with 50 μL amplex red reagent and incubated in dark at room temperature for 10 min. Following incubation, the absorbance of pink coloured-resorufin was measured at 570 nm using multi-well plate reader (Synergy LX, BioTek).

4. Generation and scavenging of singlet oxygen species

Singlet oxygen species ($^1\text{O}_2$) were generated in a 450 μl reaction system (prepared in dark environment) consisting of 0.23 μM horseradish peroxidase (HRP) and 1 μM H_2O_2 maintained in 50mM degassed sodium phosphate buffer. Singlet oxygen sensor green (SOSG) (0.55 μM) was added to the reaction system and incubated for 15 minutes.

Following incubation, the emission intensity of SOSG at 530 nm was measured at an excitation wavelength 475 nm, using the multimode reader (EnSpire, PerkinElmer). In case of kinetics study, 250 μl reaction system was prepared with 0.23 μM HRP and 0.55 μM SOSG in tris buffer and 1 μM H_2O_2 was added at the end to the reaction system prior to measuring the SOSG emission intensity at 530 nm using the multimode reader (EnSpire, PerkinElmer) at an excitation wavelength 475 nm.

The possibility of generation of superoxide radicals in the HRP + H_2O_2 system was tested in a 500 μl reaction system, consisting hypoxanthine, xanthine oxidase, catalase in sodium phosphate buffer of pH 6 with dihydroethidium (DHE) as the fluorescent probe for the detection of superoxide radicals. The fluorescent emission intensity of DHE was measured at 530 nm at an excitation wavelength 475 nm using the multimode reader (EnSpire, PerkinElmer).

4.1. Singlet oxygen scavenging activity of Dex-CeO₂ NPs and Dex-Mn₃O₄ NPs. $^1\text{O}_2$ scavenging activity of Dex-CeO₂ NPs was determined in the range 500 μM -4mM and Dex-Mn₃O₄ NPs in the range 5-200 μM . 10 μl from the corresponding stock solutions of concentration ranges of Dex-CeO₂ NPs and Dex-Mn₃O₄ NPs under study were added to the reaction system consisting 0.23 μM HRP and 1 μM H_2O_2 . Following the addition of nanoparticles, the reaction system was incubated for 5 minutes and 0.55 μM SOSG was added. After an incubation of 15 minutes, the emission intensity of SOSG was subsequently measured at 530 nm using multimode reader (EnSpire, PerkinElmer) at an excitation wavelength 475 nm.

4.2. Evaluation of singlet oxygen species generation using inhibitors. The inhibitory effect of sodium azide and parabenzoquinone on the emission intensity of SOSG at 530 nm was studied at a concentration of 125 μM and 1500 μM respectively. 125 μM sodium azide and 1500 μM parabenzoquinone were added to 250 μl reaction system with 0.23 μM HRP and 1 μM H_2O_2 respectively. Further, the emission intensity of SOSG at 530 nm was measured after an incubation of 15 minutes using the multimode reader (EnSpire, PerkinElmer) at an excitation wavelength 475 nm.

5. Redox recycling and catalytic efficiency of Dex-CeO₂ NPs

The redox recycling between the Ce³⁺ and Ce⁴⁺ oxidation states in Dex-CeO₂ NPs was evaluated in comparison with bare CeO₂ NPs. 1 mM suspension of both Dex-CeO₂ NPs and bare CeO₂ NPs were mixed with 200 μM H₂O₂ respectively, and the colour change was monitored. Both bare and Dex-CeO₂ NPs developed yellow coloration within 10 minutes of H₂O₂ addition, indicative of the oxidation of Ce³⁺ to Ce⁴⁺. The yellow suspensions were then incubated at 37 °C for 15 days. Following incubation, the suspensions reverted to a colourless state, suggesting the regeneration of Ce³⁺. Further to confirm redox recyclability, H₂O₂ (200 μM) was reintroduced to the regenerated suspensions, and the reappearance of yellow coloration was observed, indicating a second cycle of Ce³⁺ oxidation to Ce⁴⁺. The catalytic scavenging activity ([•]OH and ¹O₂) of Dex-CeO₂ NPs before and after the redox recycling was assessed using the highest concentrations, 2.5 mM and 4 mM. In addition, the UV-Vis absorbance spectra of both bare and Dex-CeO₂ NPs were recorded before and after redox recycling.

6. Biocompatibility assessment of nanoparticles

6.1 Assessment of nanozyme stability in cell culture media.

Dex-CeO₂ and Dex-Mn₃O₄ NPs (1 mM) were incubated in serum-free and serum-containing DMEM/F12 medium for 24 hours at room temperature. Post-incubation in serum-free and serum-containing DMEM/F12 medium, both nanozymes were evaluated for [•]OH and ¹O₂ scavenging activities to assess for potential alterations in enzymatic activity.

6.2. Cell line cultivation

The intestinal epithelial cells (IEC-6) were purchased from the NCCS, Pune. The cells were cultured in DMEM-F12 medium supplemented with 10% FBS and 1% antibiotic and antimycotic solution under conditions of 5% CO₂ and 95% humidity in a CO₂ incubator.

6.3. Cell viability assay

About 1 x 10⁴ cells/well were seeded in 96 well plate and incubated overnight to adhere. Next day, the cells were exposed to varying concentration of Dex-CeO₂ NPs and Dex-Mn₃O₄ NPs (0.1 μg/mL, 0.25 μg/mL, 0.5 μg/mL, 0.75 μg/mL, 1μg/mL) and further

incubated for different durations (24 hr, 48 hr and 72 hr). After the specified incubation period, MTT dye (0.5 mg/mL) was added and incubated for 4 hours before dissolving the formazan crystal in DMSO. The O.D. was recorded at 575 nm using Synergy LX, BioTek, Agilent.

6.4. Assessment of ROS generation. About 2×10^4 cells/well were seeded on coverslip in 12 well plate and allowed to adhere overnight. Next day, the cells were treated with different concentrations of Mn_3O_4 NPs (0.75 $\mu\text{g/mL}$, 1 $\mu\text{g/mL}$) and incubated for 24 hours. As a control, H_2O_2 (20 μM) was incubated for 30 min. Post incubation, treatment was removed and cells were incubated with H_2DCFDA (20 μM) dye for 30 min, washed with 1 x PBS (twice) and then stained with DAPI (2.5 $\mu\text{g/mL}$) for 15 min. Post staining, cells were washed with 1 x PBS (thrice) and mounted on glass slide using gold antifade mounting medium. The slides were stored at 4 °C until observed under fluorescence microscope using green channel (Ex/Em: 480/530 nm) (Axiocam, ZEISS).

6.5. Cell cycle analysis

1×10^5 cells per well was seeded in 12 well plate and incubated overnight, Next day, cells were treated with different concentrations of Dex- CeO_2 NPs and Dex- Mn_3O_4 NPs (0.75 $\mu\text{g/mL}$, 1 $\mu\text{g/mL}$) and incubated for 24 hours. Post-incubation, cells were harvested using trypsin-EDTA, treated with 70% ethanol (ice-cold) for 30 min and further incubated with lysis buffer (0.25% Triton-X in PBS) for 30 min. Subsequently, the cells were incubated with 20 $\mu\text{g/mL}$ RNaseA for 30 min, stained with 20 $\mu\text{g/mL}$ PI for 10 min and analysed using a flow cytometer (BD FACSMelody™) to measure the cell cycle by detecting PI dye. A histogram of cell number against PI intensity was made to determine the ratio of cells under G1 (2n), S (2n+), and G2/M phase (4n).

Table S1. Binding energies and integrated areas of the deconvoluted spin-orbit peak pairs in the Ce 3d core-level spectrum

Oxidation State	Peak	BE (eV)	Area under the peak	Sum of the area
Ce ⁺³	3d _{3/2}	900.75	3915.79	8798.12
	3d _{5/2}	881.4	4882.33	
'Ce ⁺³	3d _{3/2}	906.01	1179.217	4169.447
	3d _{5/2}	886.18	2990.23	
Ce ⁺⁴	3d _{3/2}	915.25	3221.515	6836.12
	3d _{5/2}	896.85	3614.605	

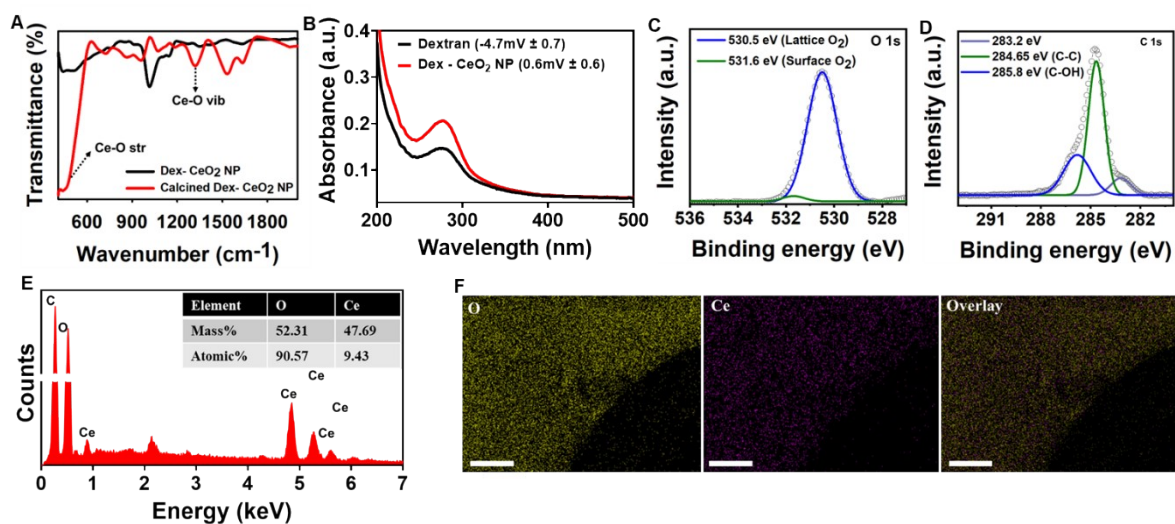


Fig. S1. Characterization of Dex-CeO₂ NPs: (A) FTIR spectra of pristine (black) and calcined Dex-CeO₂ NPs (red), (B) UV-Visible spectra of dextran (black curve) and Dex-CeO₂ NPs (red curve) – inset shows the zeta potential of dextran and pristine Dex-CeO₂ NPs, O 1s (C) and C 1s (D) XPS spectra recorded from Dex-CeO₂ NPs (E) EDX spectra of Dex-CeO₂ NPs, and (F) corresponding elemental mapping of the area showing the signals of ‘O’, ‘Ce’ and the overlay profile of elements (Scale bar = 4 μm).

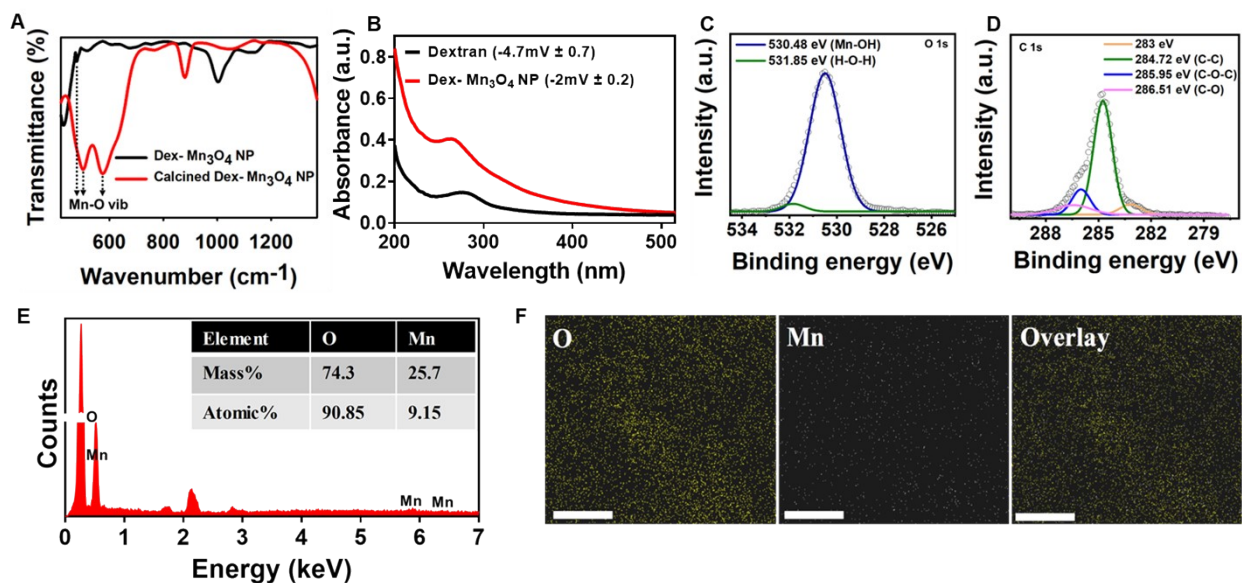


Fig. S2. Characterization of Dex-Mn₃O₄ NPs: (A) FTIR spectra of as synthesized (black) and calcined Dex-Mn₃O₄ NPs (red), (B) UV-Visible spectra of dextran (black curve) and Dex-Mn₃O₄ NPs (red curve) – inset shows the zeta potential of dextran and as synthesized Dex-Mn₃O₄ NPs, O 1s (C) and C 1s (D) XPS spectra recorded from Dex-Mn₃O₄ NPs (E) EDX spectra of Dex-Mn₃O₄ NPs, and (F) corresponding elemental mapping of the area showing the signals of ‘O’, ‘Mn’ and the overlay profile of elements (Scale bar = 4 μm).

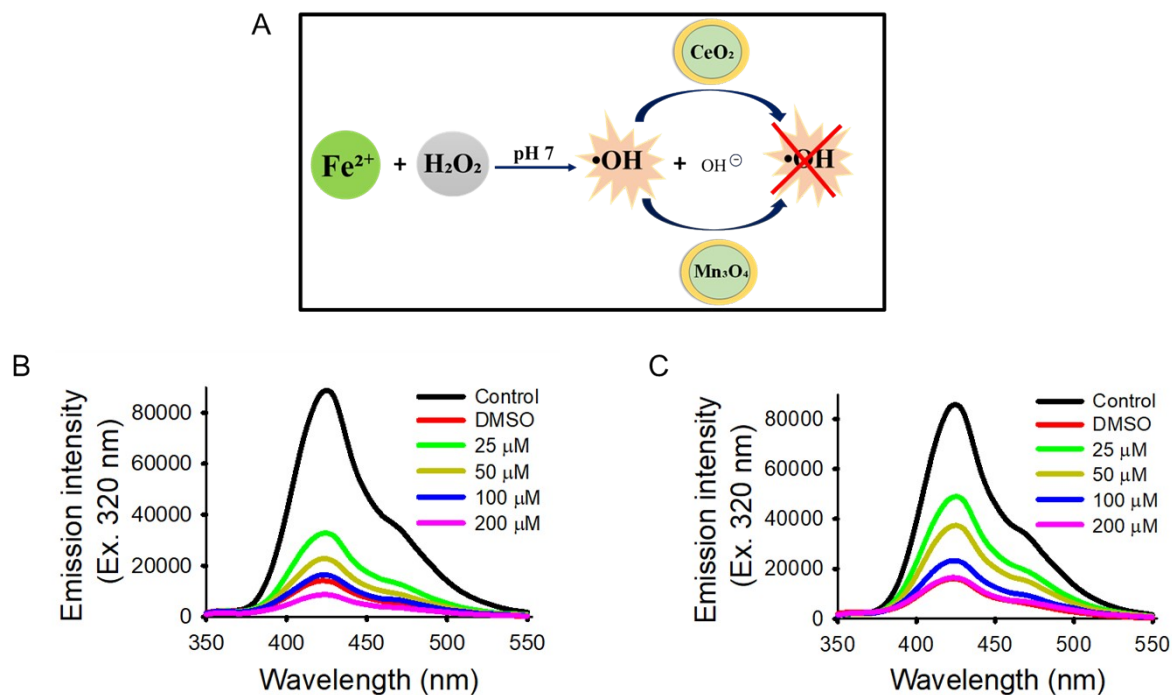


Fig. S3. $\cdot\text{OH}$ scavenging by Dex- CeO_2 NPs and Dex- Mn_3O_4 NPs: (A) Schematic representation showing the generation of $\cdot\text{OH}$ via the Fenton reaction and subsequent scavenging by Dex- CeO_2 NPs and Dex- Mn_3O_4 NPs, Fluorescence emission spectra of oxidised TA (by $\text{FeSO}_4 + \text{H}_2\text{O}_2$) showing reduction in emission intensity with increasing concentrations of (B) Dex- CeO_2 NPs and (C) Dex- Mn_3O_4 NPs in the range 25- 200 μM . All the experiments have been performed three times independently, and the data is plotted with standard deviation wherever applicable.

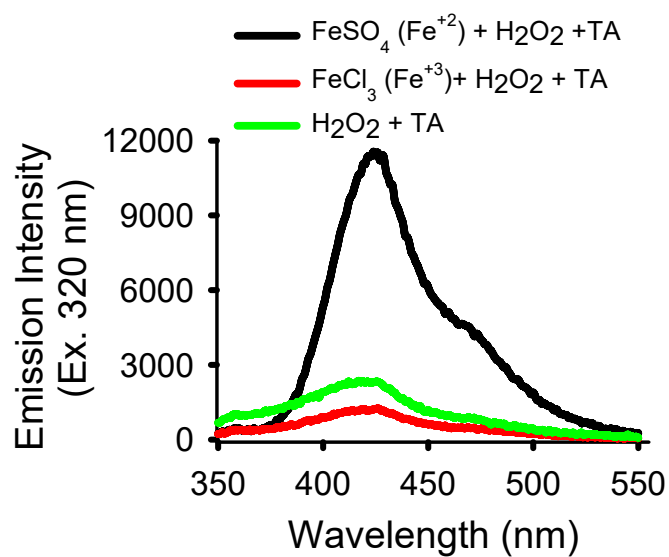


Fig. S4. Evaluating the possibility of oxidation of TA by only H₂O₂. TA oxidation reaction was performed by replacing FeSO₄ (Fe²⁺) with FeCl₃ (Fe³⁺) in the Fenton reaction system (red curve), and direct exposure of TA to H₂O₂ (green curve), with respect to the control consisting of FeSO₄, H₂O₂, and TA (black curve).

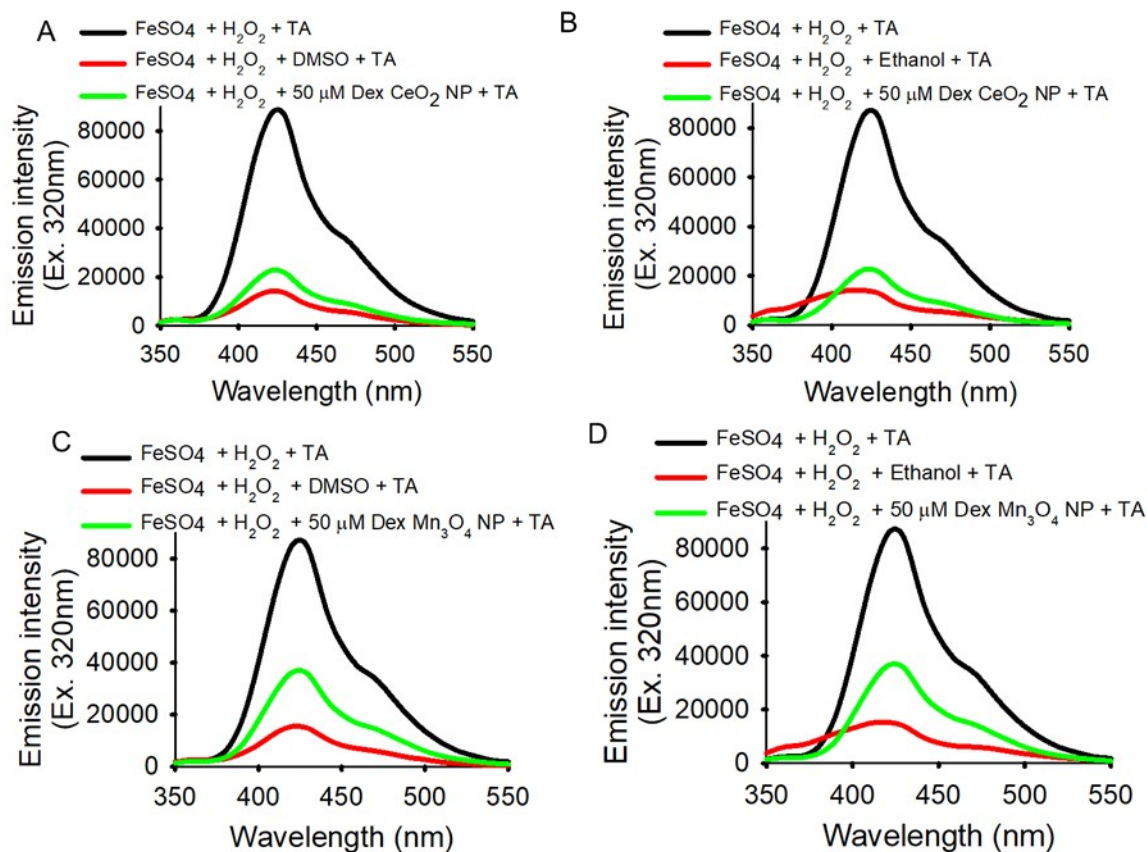


Fig. S5. Scavenging of $\cdot\text{OH}$ by Dex- CeO_2 NPs and Dex- Mn_3O_4 NPs and comparison with different inhibitors: Emission spectra of oxidized TA (by $\text{FeSO}_4 + \text{H}_2\text{O}_2$, black curve) in comparison with the presence of (A) DMSO (red curve) and $50 \mu\text{M}$ Dex- CeO_2 NPs (green curve), (B) ethanol (red curve) and $50 \mu\text{M}$ Dex- CeO_2 NPs (green curve), (C) DMSO (red curve) and $50 \mu\text{M}$ Dex- Mn_3O_4 NPs (green curve) and (D) ethanol (red curve) and $50 \mu\text{M}$ Dex- Mn_3O_4 NPs (green curve). All the experiments have been performed three times independently, and the data is plotted with standard deviation wherever applicable.

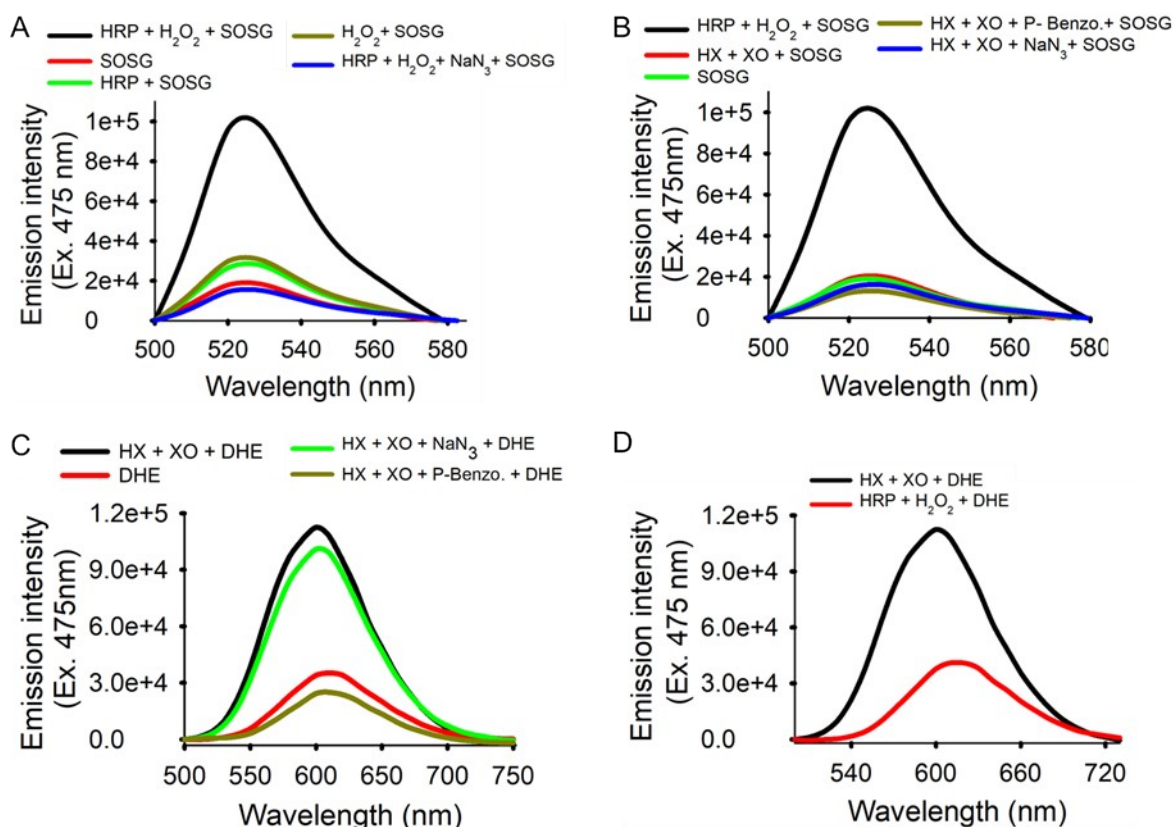


Fig. S6. $^1\text{O}_2$ generation in HRP + H_2O_2 system: (A) Fluorescence emission spectra of SOSG showing the generation of $^1\text{O}_2$, (B) Comparison of the insignificant emission intensity of oxidised SOSG in hypoxanthine (HX) + xanthine oxidase (XO) system with respect to HRP + H_2O_2 system, (C) Emission intensity of dihydroethidium (DHE) on exposure to NaN_3 and P-Benzo. (D) Emission intensity of DHE in HRP + H_2O_2 system in comparison with HX + XO system. All the experiments have been performed three times independently, and the data is plotted with standard deviation wherever applicable.

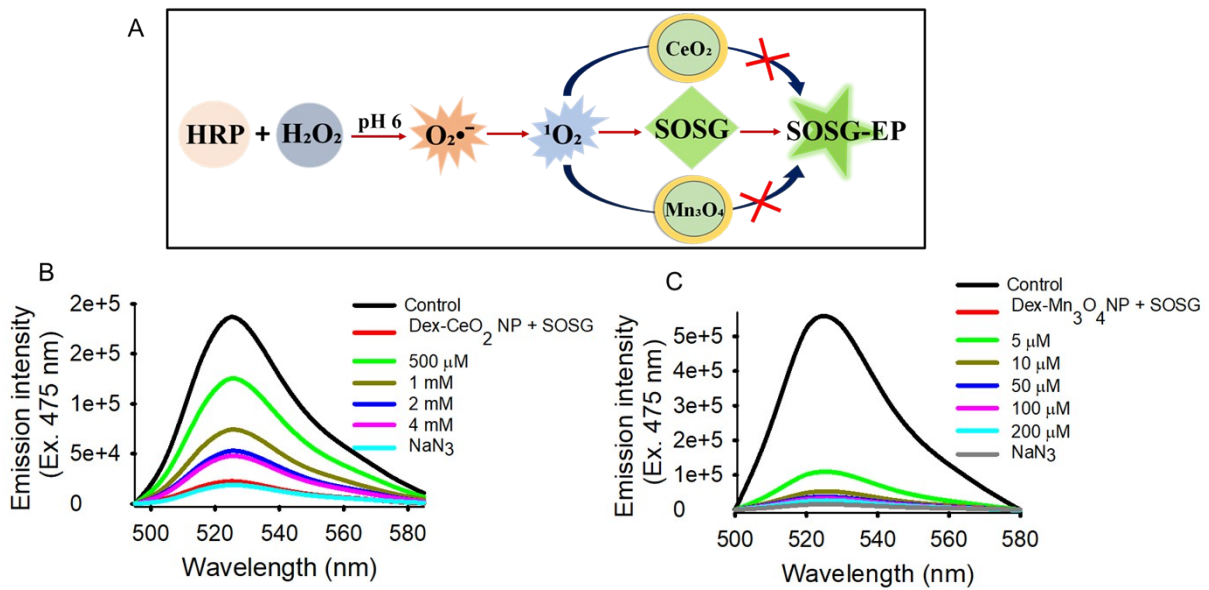


Fig. S7. ¹O₂ generation and scavenging by Dex-CeO₂ NPs and Dex-Mn₃O₄ NPs: (A) Schematic representation of ¹O₂ formation in HRP + H₂O₂ system and scavenging by Dex-CeO₂ NPs and Dex-Mn₃O₄ NPs, Concentration dependent decline in the emission intensity of oxidized SOSG with increasing concentration of (B) Dex-CeO₂ NPs and (C) Dex-Mn₃O₄ NPs compared to the control (HRP + H₂O₂ + SOSG). All the experiments have been performed three times independently, and the data is plotted with standard deviation wherever applicable.

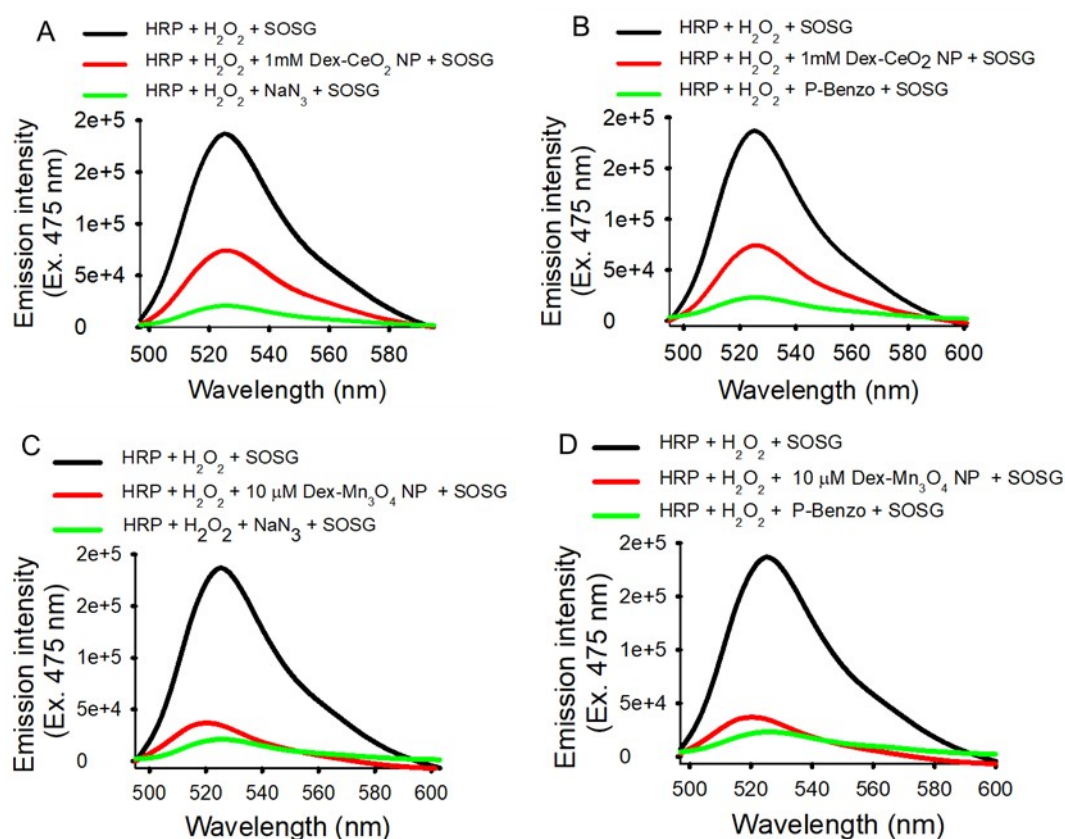


Fig. S8. Comparative analysis of ¹O₂ scavenging efficiency between specific inhibitors and the nanozymes (Dex-CeO₂ NPs and Dex-Mn₃O₄ NPs): Fluorescence spectra showing comparative reduction in emission intensity of oxidised SOSG in presence of inhibitors, (A) NaN₃ and 1mM Dex-CeO₂ NP, (B) Para-benzoquinone and 1mM Dex-CeO₂ NPs, (C) NaN₃ and 10 μM Dex-Mn₃O₄ NPs, (D) P-Benzo and 10 μM Dex-Mn₃O₄ NPs. All the experiments have been performed three times independently, and the data is plotted with standard deviation wherever applicable.

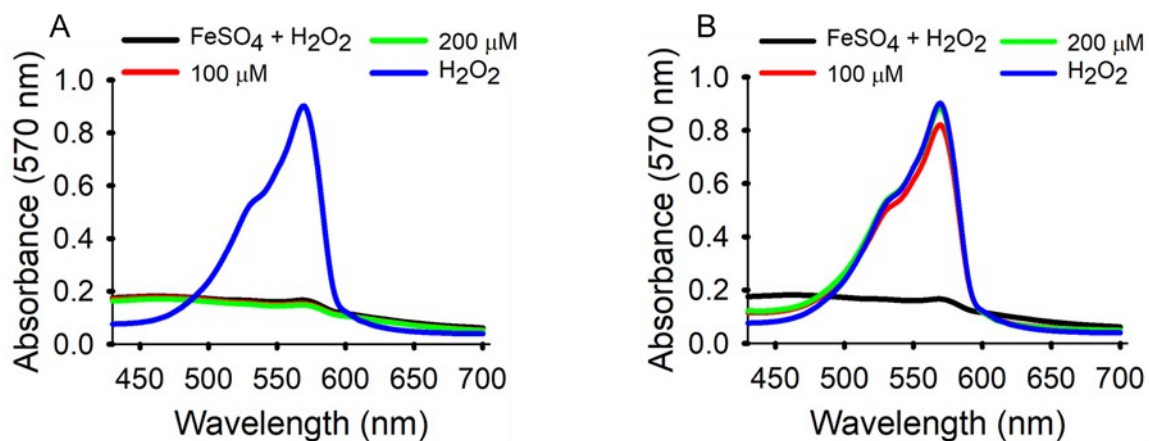


Fig. S9. Testing for the generation of H_2O_2 in the supernatant of the Fenton reaction system used to evaluate $\cdot\text{OH}$ scavenging activity of Dex- CeO_2 and Dex- Mn_3O_4 NPs by amplex red assay: H_2O_2 generation leads to oxidation of the amplex red to form resorufin. Comparison of the absorbance spectra of resorufin at 570 nm between (A) Dex- CeO_2 NPs and (B) Dex- Mn_3O_4 NPs with respect to the control ($\text{FeSO}_4 + \text{H}_2\text{O}_2$, black curve) and H_2O_2 (blue curve). All the experiments have been performed three times independently, and the data is plotted with standard deviation wherever applicable.

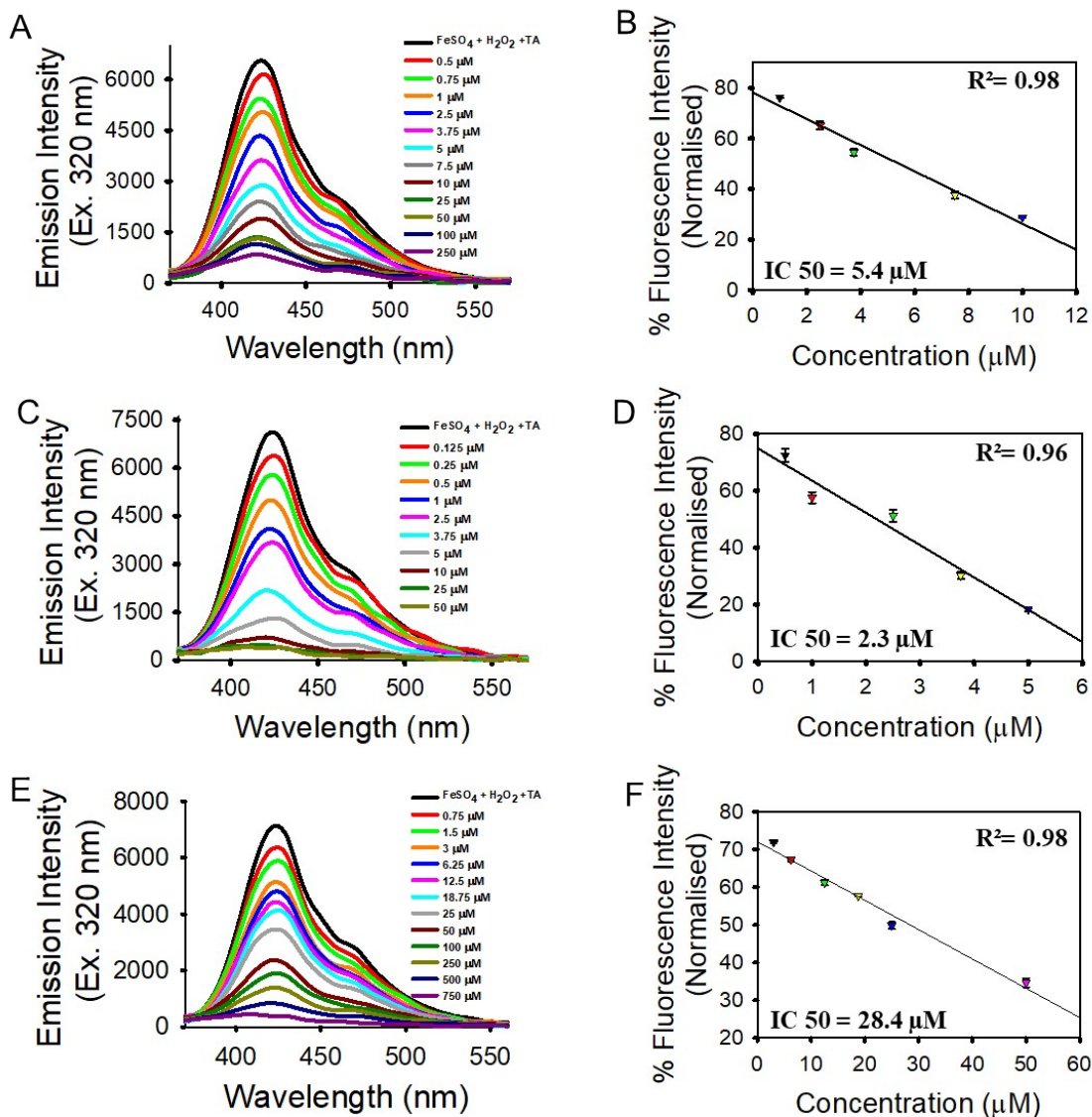


Fig. S10. Comparative analysis of the IC₅₀ values of ·OH scavenging by nanozymes (Dex-CeO₂ NPs and Dex-Mn₃O₄ NPs) and N-Acetyl Cysteine (NAC): Emission spectra of oxidized TA showing reduction in emission intensity with increasing concentration of (A) Dex-CeO₂ NPs and (B) the representative standard curve plotted between emission intensity and concentration for IC₅₀ determination, (C) Dex-Mn₃O₄ NPs and (D) the representative standard curve, (E) NAC and (F) the representative standard curve. All the experiments have been performed three times independently, and the data is plotted with standard deviation wherever applicable.

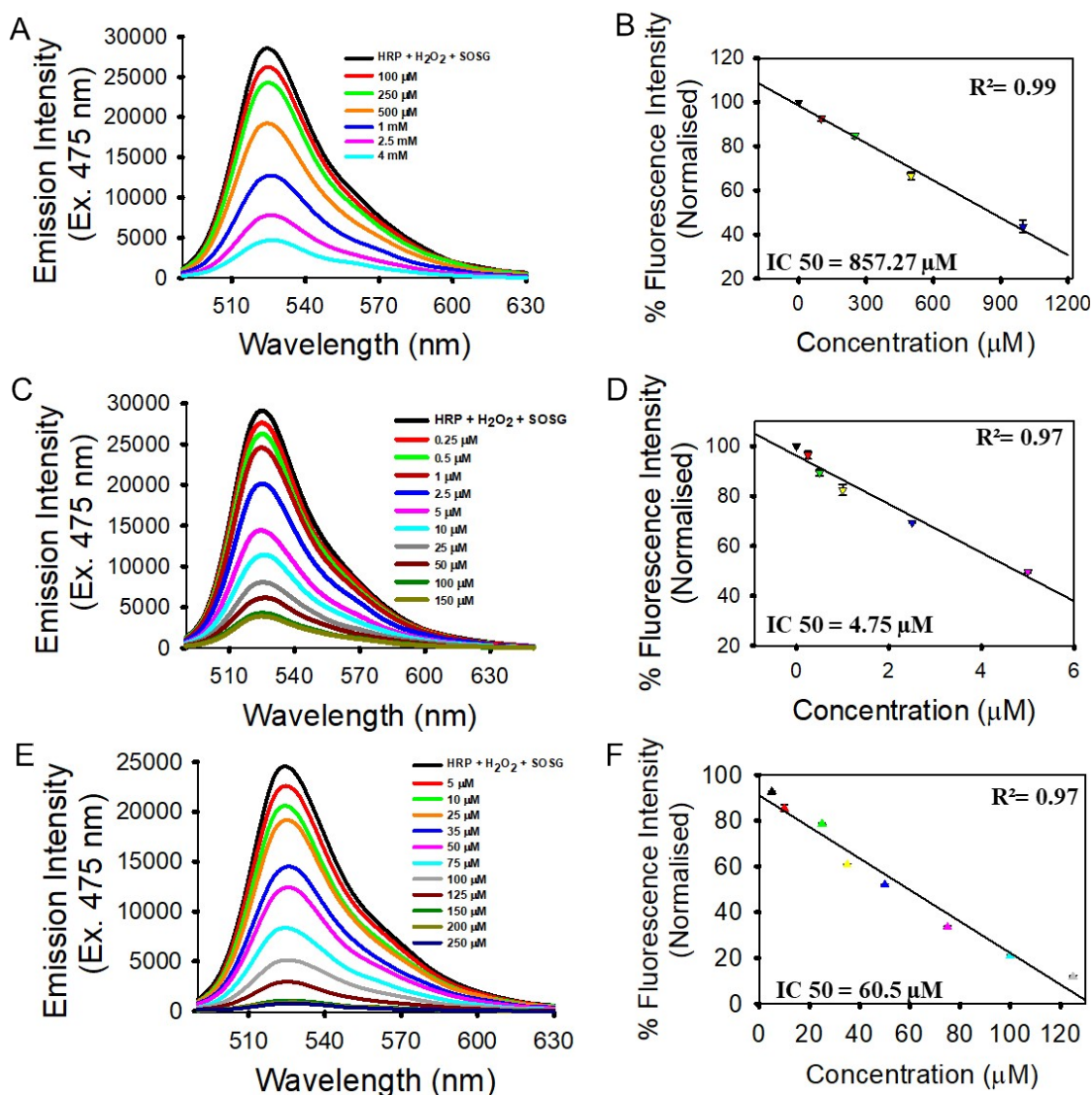


Fig. S11. Comparative analysis of the IC_{50} values of 1O_2 scavenging by nanozymes (Dex- CeO_2 NPs and Dex- Mn_3O_4 NPs) and NaN_3 : Emission spectra of oxidized SOSG showing reduction in emission intensity with increasing concentration of (A) Dex- CeO_2 NPs and (B) the representative standard curve plotted between emission intensity and concentration for IC_{50} determination, (C) Dex- Mn_3O_4 NPs and (D) the representative standard curve, (E) NaN_3 and (F) the representative standard curve. All the experiments have been performed three times independently, and the data is plotted with standard deviation wherever applicable.

Table S2. IC₅₀ values of nanozymes and specific inhibitors for $\cdot\text{OH}$ and $^1\text{O}_2$ scavenging

Scavenging radical	Nanoparticle/ Scavenger	IC₅₀ (μM)
$\cdot\text{OH}$	Dex-CeO ₂ NPs	5.4 μM
	Dex-Mn ₃ O ₄ NPs	2.3 μM
	NAC	28.4 μM
$^1\text{O}_2$	Dex-CeO ₂ NPs	857.27 μM
	Dex-Mn ₃ O ₄ NPs	4.75 μM
	NaN ₃	60.5 μM

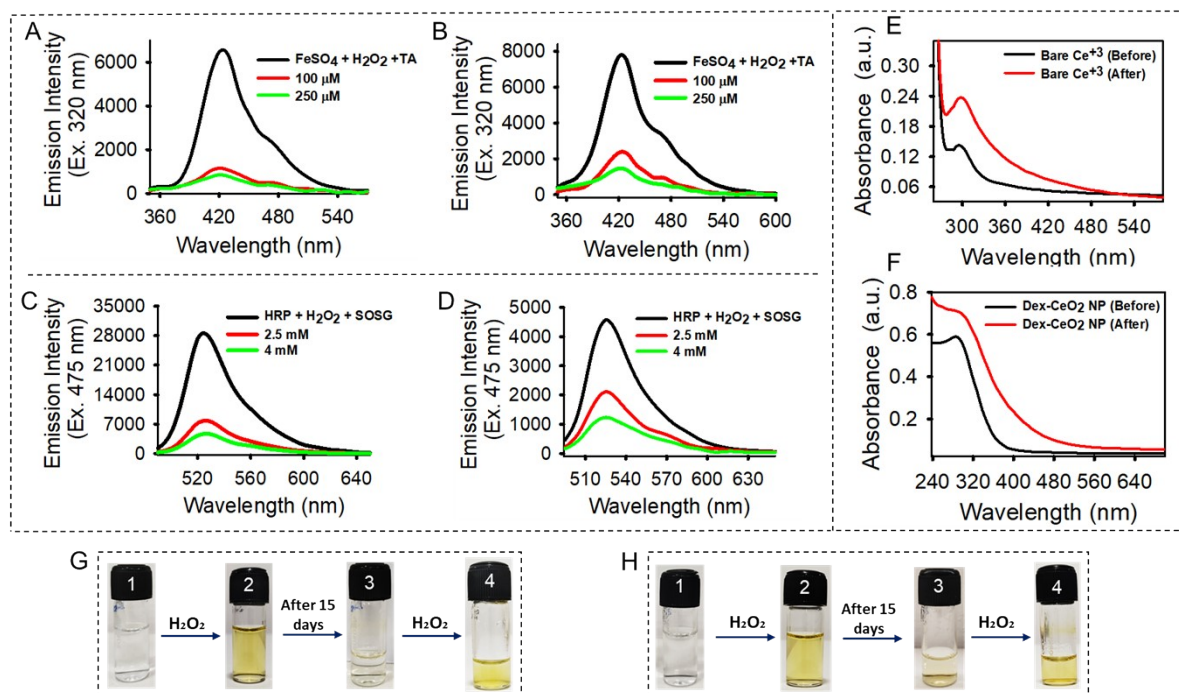


Fig. S12. Redox cycling and sustained enzymatic activity in Dex-CeO₂ NPs: (A) $\cdot\text{OH}$ scavenging activity of Dex-CeO₂ NPs (A) before and (B) after redox recycling. $^1\text{O}_2$ scavenging activity of Dex-CeO₂ NPs (C) before and (D) after redox recycling. UV-Vis absorbance spectra of (E) bare-CeO₂ NPs and (F) Dex-CeO₂ NPs before and after redox recycling. Redox recycling in bare-CeO₂ NPs (G, bottle 1) and Dex-CeO₂ NPs (H, bottle 1) is demonstrated by the oxidation of Ce³⁺ to Ce⁴⁺ (yellow colour) (G, bottle 2 and H, bottle 2) and regeneration of Ce³⁺ (colourless) (G, bottle 3 and H, bottle 3) following 15 days incubation after H₂O₂ addition. A second cycle of redox recycling is demonstrated by the development of yellow colour after addition of H₂O₂ in the regenerated colourless suspension of bare-CeO₂ NPs (G, bottle 4) and Dex-CeO₂ NPs (H, bottle 4).

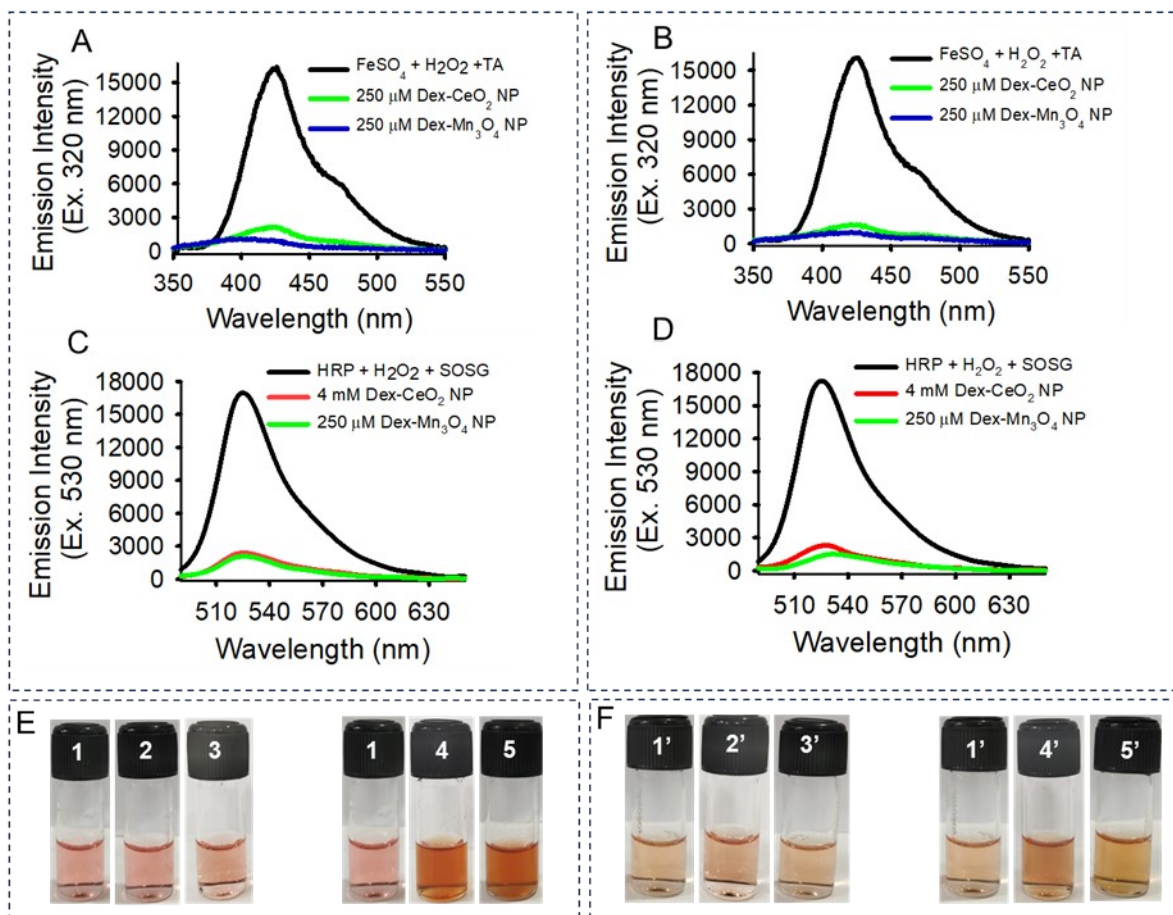


Fig. S13. Stability assessment of the Dex-CeO₂ NPs and Dex-Mn₃O₄ NPs in serum free and serum containing cell culture media: [•]OH scavenging activity of Dex-CeO₂ NPs and Dex-Mn₃O₄ NPs following 24-hour incubation in (A) incomplete media (DMEM-F12) and (B) complete media (DMEM-F12 + FBS). ¹O₂ scavenging activity of Dex-CeO₂ NPs and Dex-Mn₃O₄ NPs following 24-hour incubation in (C) incomplete media (DMEM-F12) and (D) complete media (DMEM-F12 + FBS). (E, bottle 1 - Incomplete media, bottle 2- Incomplete media + freshly added Dex-CeO₂ NPs, bottle 3 - 24-hours incubated Dex-CeO₂ NPs in incomplete media, bottle 4- Incomplete media + freshly added Dex-Mn₃O₄ NPs, bottle 5- 24-hours incubated Dex-Mn₃O₄ NPs in incomplete media), (F, bottle 1' - Complete media, bottle 2' - Complete media + freshly added Dex-CeO₂ NPs, bottle 3' - 24-hours incubated Dex-CeO₂ NPs in complete media, bottle 4' - Complete media + freshly added Dex-Mn₃O₄ NPs, bottle 5' - 24-hours incubated Dex-Mn₃O₄ NPs in complete media).

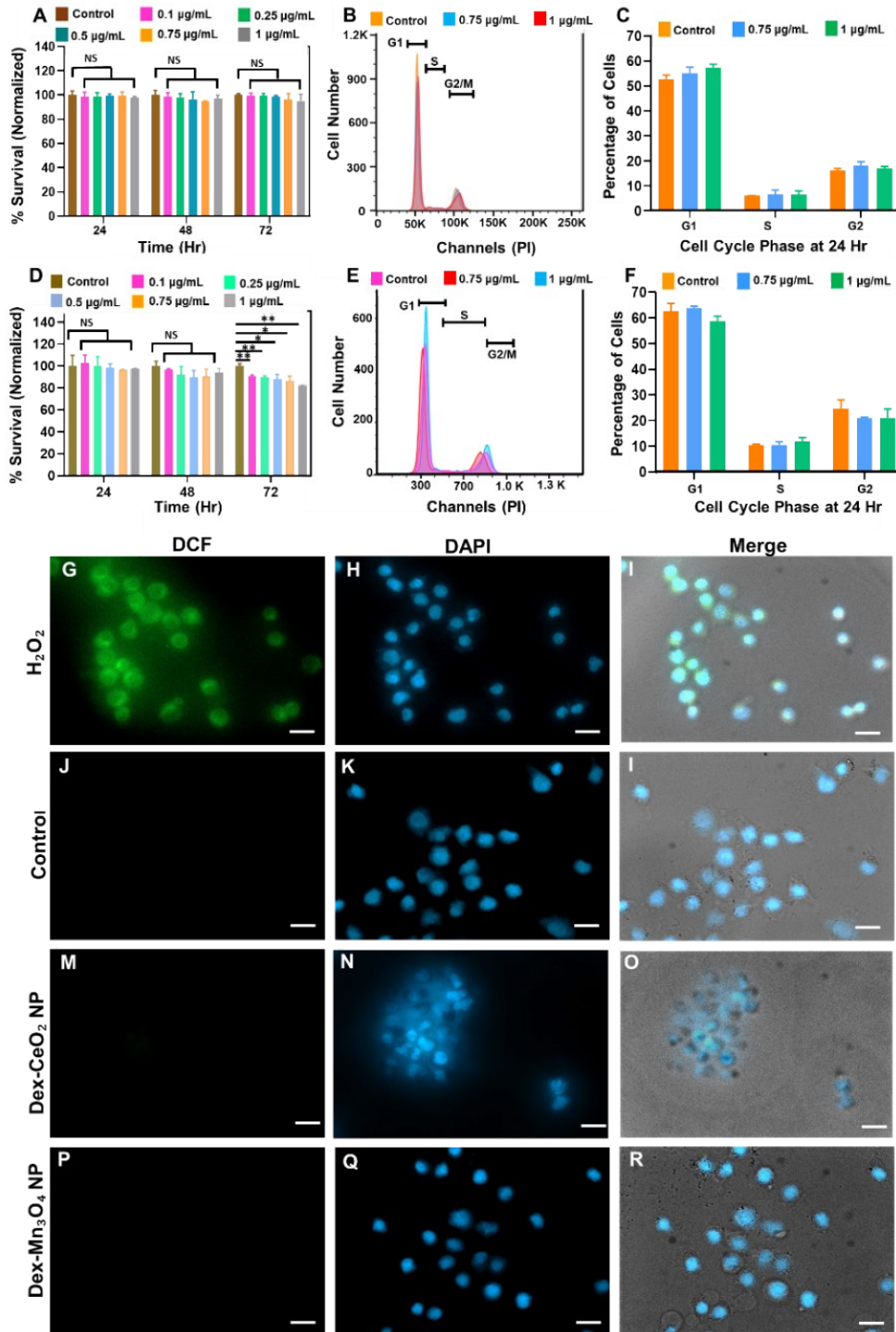


Fig. S14. Biocompatibility evaluation of Dex-CeO₂ NPs and Dex-Mn₃O₄ NPs in IEC6 cells: MTT assay testing the effect of (A) Dex-CeO₂ NPs and (D) Dex-Mn₃O₄ NPs on intestinal epithelial cell line (IEC-6) at different concentrations (0.1 µg/mL, 0.25 µg/mL, 0.5 µg/mL, 0.75 µg/mL, 1 µg/mL) for 24 hr, 48 hr and 72 hr. Cell cycle analysis of IEC-6 cell line after treating with (B) Dex-CeO₂ NPs and (E) Dex-Mn₃O₄ NPs. Quantification of cell cycle assay of IEC-6 cell line after treating with (C) Dex-CeO₂ NPs and (F) Dex-Mn₃O₄ NPs. Fluorescence

microscopy images representing the ROS generation in IEC-6 cell line after treating with H₂O₂ for 30 min (G-I) and subsequent scavenging with Dex-CeO₂ NPs (M-O) and Dex-Mn₃O₄ NPs (P-R) at a concentration of 1 μg/mL for 24 hr respective to untreated control cells (J-L). Data is expressed as mean ± SD of three different experiments. Survival % of IEC-6 cells are expressed relative to untreated controls (significance value, *p < 0.05, ** p < 0.01). Scale bar = 50 μm.

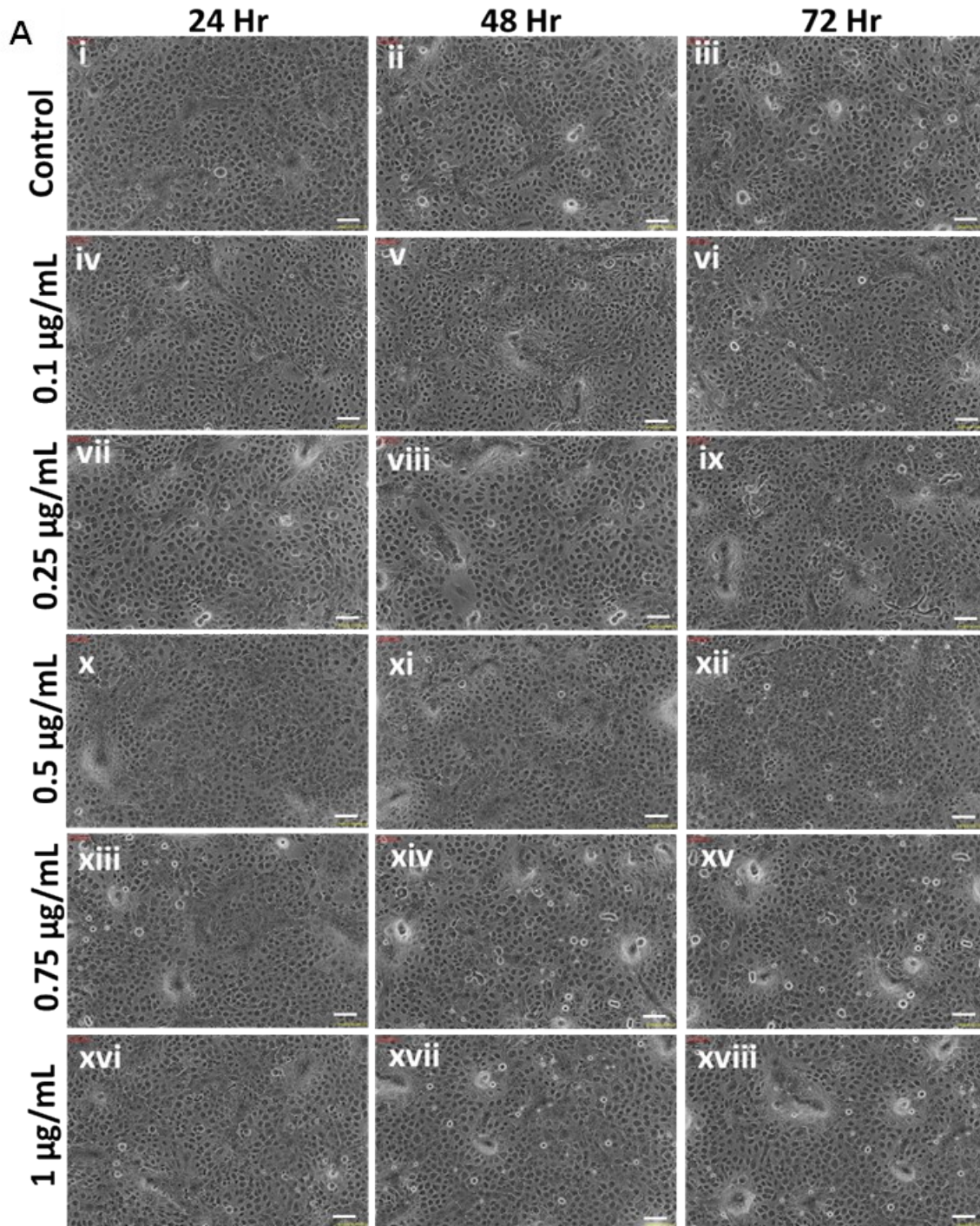


Fig. S15. *In vitro* cytotoxicity assays to study the effect of Dex-CeO₂ NPs on IEC-6 cell line. (A) Microscopic images of IEC-6 cells after treating with different concentrations of Dex-CeO₂ NPs (0.1 $\mu\text{g/mL}$, 0.25 $\mu\text{g/mL}$, 0.5 $\mu\text{g/mL}$, 0.75 $\mu\text{g/mL}$, 1 $\mu\text{g/mL}$) for 24 hr, 48 hr and 72 hr.

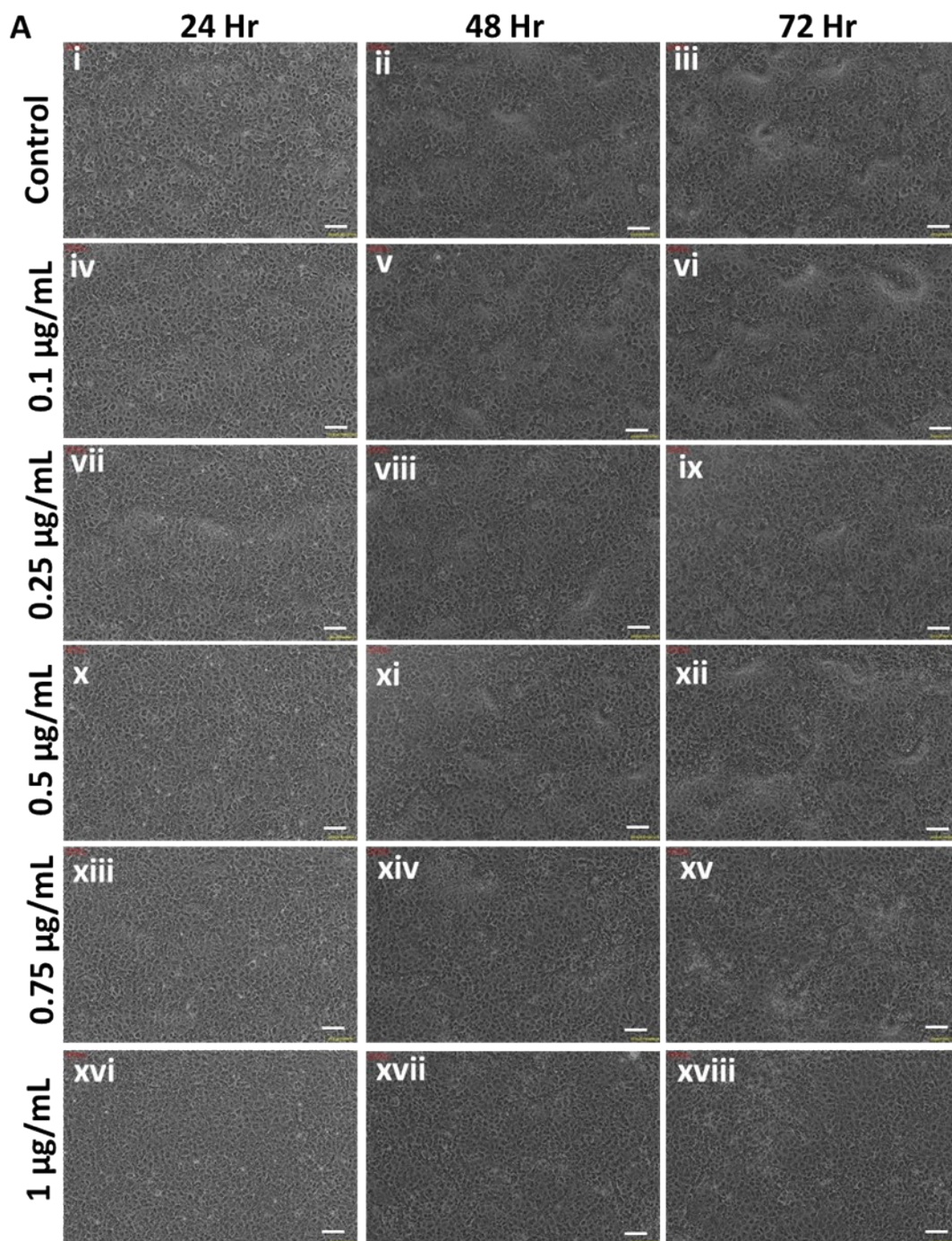


Fig. S16. *In vitro* cytotoxicity assay to study the effect of Dex-Mn₃O₄ NPs on IEC-6 cell line. (A) Microscopic images of IEC-6 cells after treating with different concentrations of Dex-Mn₃O₄ NPs (0.1 $\mu\text{g/mL}$, 0.25 $\mu\text{g/mL}$, 0.5 $\mu\text{g/mL}$, 0.75 $\mu\text{g/mL}$, 1 $\mu\text{g/mL}$) for 24 hr, 48 hr and 72 hr.

References

1. P. C. Naha, J. C. Hsu, J. Kim, S. Shah, M. Bouché, S. Si-Mohamed, D. N. Rosario-Berrios, P. Douek, M. Hajfathalian and P. Yasini, *ACS nano*, 2020, **14**, 10187-10197.
2. P. Jain, S. Bhagat, L. Tunki, A. K. Jangid, S. Singh, D. Pooja and H. Kulhari, *ACS Applied Materials & Interfaces*, 2020, **12**, 10170-10182.